

Layers update of neural network control via event-triggering mechanism *

S. Tarbouriech, C. De Souza, A. Girard

Abstract The chapter deals with the design of event-triggering mechanisms (ETM) for discrete-time linear systems stabilized by neural network controllers. The proposed event-triggering mechanism is based on the use of local sector conditions related to the activation functions, to reduce the computational cost associated with the neural network evaluation. Such a mechanism avoids redundant computations by updating only a portion of the layers instead of evaluating periodically the complete neural network. Sufficient matrix inequality conditions are provided to design the parameters of the event-triggering mechanism and compute an inner-approximation of the region of attraction for the feedback system. The theoretical conditions are obtained by using a quadratic Lyapunov function and an adequate abstraction of the activation functions via generalised sector condition to decide whether the outputs of the layers should be transmitted through the network or not. Convex optimisation procedures can be associated to the theoretical conditions in order to maximise the approximation of the region of attraction or to minimise the number of updates. The advantages and the drawbacks of our approach are illustrated in an example borrowed from the literature, namely the nonlinear inverted pendulum system stabilized by a trained neural network.

S. Tarbouriech

LAAS-CNRS, Université de Toulouse, CNRS, Toulouse, France, e-mail: tarbour@laas.fr

C. De Souza

Leyfa Measurement une filiale SNCF, Aucamville, France, e-mail: carla.souza93@hotmail.com

A. Girard

Université Paris-Saclay, CNRS, CentraleSupélec, Laboratoire des Signaux et Systèmes, 91190, Gif-sur-Yvette, France, e-mail: antoine.girard@l2s.centralesupelec.fr

* This work has been supported by ANR under the project HANDY number 18-CE40-0010.

1 introduction

The use of neural networks (NNs) for control purpose is attracting a lot of works, in particular, due to recent advancements in deep learning. Indeed, NNs may replace some existing computationally expensive controllers typically as model predictive controllers (MPCs), requiring online solutions to an optimal control problem. Thus, NNs allow for an efficient and inexpensive embedded implementation [9], [28], [13]. However, NN controllers lack guarantees, which typically restrict their use in safety-critical applications such as for example in surgical procedures, and medical support systems [24]. Therefore, the ability to develop tools that can provide useful certificates of stability, safety, and robustness for NN controlled systems appears as a crucial direction of research. One can cite several works studying different aspect as verifying such systems. [5], [17], [15], [14], [21].

From a control point of view, the structures of NNs are interesting due to various types of nonlinear activation functions, potentially numerous layers, and a large number of hidden neurons. Furthermore, the adaptation of Lyapunov theory and the development of diverse ways to embed the nonlinear activation functions is a very exciting prospective. Hence, the use of adequate quadratic constraints (QCs) allowing to handle the nonlinear activation functions has been considered in different contexts: [4] checked the safety of NNs by using QCs to outer-bound their outputs given a set of inputs. [25] combined Lyapunov theory with local sector QCs to analyze the stability of feedback systems with neural network controllers. [16] analyzed stability in offset-free setpoint tracking with a piecewise constant reference. [12] proposed QCs based on partial gradients to certify the input-output stability of reinforcement-learning (RL) controlled systems.

Moreover, in the context of network control systems it is important not only to satisfy some control requirements but also to alleviate the communication network consumption. A pertinent alternative control paradigm to reduce the computational overhead and communication traffic, thus saving the limited network resources consists in event-triggered control (ETC) strategy. Such a strategy allows to update the control only when necessary (corresponding to a predefined mechanism), which is different from executing control tasks at periodic intervals. Then, the ETC approach describes a mechanism to determine the sampling instants without compromising the desired system performance (see, for example, [8, 20, 7, 3]). In the particular context of neural networks, the ETC technique has been mainly used to transmit states during the learning process, as, for example, studied in [18], [23], [29], [6].

Taking inspiration from our previous work [1], in this chapter, we consider that the neural network has already been trained and we design an event-triggering mechanism (ETM) to transmit the output of the layers, to reduce the computational cost associated with the control law evaluation. The ETM we investigate in this chapter uses the knowledge on the nonlinear activation functions, which are supposed to be saturation functions. We then take advantage of less conservative conditions to deal with saturation functions [22] and we propose an ETM based on a local sector conditions satisfied by the activation functions to decide whether the outputs of the layers should be transmitted through the network or not. We use quadratic constraints

(QCs) not only to abstract the nonlinear activation functions but also to model the event-triggering rule. Hence, considering discrete-time linear time-invariant (LTI) plants stabilized by known neural network controllers, combining Lyapunov theory and generalized sector condition, we develop sufficient matrix inequalities conditions to compute the triggering parameters and characterize an estimate of the domain of attraction for the feedback system. An optimization scheme incorporating these conditions is also established to effectively reduce the update of the neural network layers. An example borrowed from the literature is used to illustrate the effectiveness of the proposal.

Notation. \mathbb{N} , \mathbb{R}^n , $\mathbb{R}^{n \times m}$ denote respectively the sets of nonnegative integers, n -dimensional vectors and $n \times m$ matrices. $\mathbb{D}_{>0}^n$ (respectively $\mathbb{D}_{\geq 0}^n$) is the set of diagonal positive definite (respectively, positive semi-definite) matrices of dimension n . For any matrix A , A^\top denotes its transpose. For any square matrix A , $\text{trace}(A)$ denotes its trace and $He\{A\} = A + A^\top$. $\text{diag}(A_1, A_2)$ is a block-diagonal matrix with block diagonal matrices A_1 and A_2 . For two symmetric matrices of same dimensions, A and B , $A > B$ means that $A - B$ is symmetric positive definite. \mathbf{I} and $\mathbf{0}$ stand respectively for the identity and the null matrix of appropriate dimensions. For a partitioned matrix, the symbol \star stands for symmetric blocks. For any vector $x \in \mathbb{R}^n$ and any symmetric positive definite (or semi-positive definite) matrix, $\|x\|_Q^2$ denotes the quadratic form $x^\top Q x$.

2 Modelling and Problem Statement

In this chapter, we consider a nonlinear control system described by the connection of a linear plant and an event-triggered neural network controller π_{ETM} . The objective is then to design an event-triggering mechanism to reduce the computational cost associated with the neural network evaluation. The following section presents the complete system under consideration.

2.1 Model Description

The plant under consideration is a discrete-time linear time-invariant (LTI) system defined by:

$$x(k+1) = A_p x(k) + B_p u(k), \quad (1)$$

where $x(k) \in \mathbb{R}^{n_p}$ is the state vector and $u(k) \in \mathbb{R}^{n_u}$ is the control input. Matrices A_p and B_p of appropriate dimensions are supposed to be constant and known. π_{ETM} is an ℓ -layer, event-triggered feedforward neural network (NN) described by:

$$\begin{aligned}
\hat{\omega}^0(k) &= x(k), \\
v^i(k) &= W^i \hat{\omega}^{i-1}(k) + b^i, \quad i \in \{1, \dots, \ell\}, \\
\omega^i(k) &= \text{sat}(v^i(k)), \\
u(k) &= W^{\ell+1} \hat{\omega}^\ell(k) + b^{\ell+1} + Kx(k),
\end{aligned} \tag{2}$$

where $v^i \in \mathbb{R}^{n_i}$ is the input to the i^{th} activation function, $\omega^i \in \mathbb{R}^{n_i}$ and $\hat{\omega}^i \in \mathbb{R}^{n_i}$ are the current output and the last forwarded output from the i^{th} layer, respectively. The activation function is a saturation map $\text{sat}(\cdot)$, which is applied element-wise and corresponds to the classical decentralized and symmetric saturation function:

$$\text{sat}(v_j^i(k)) = \text{sign}(v_j^i(k)) \min(|v_j^i(k)|, \bar{v}_j^i), \tag{3}$$

where v_j^i is the j^{th} component of v^i , and $\bar{v}_j^i > 0$, $i \in [1, \ell]$, $j \in [1, n_i]$, is the level of the saturation ($\bar{v}_j^i = -\bar{v}_j^i$). As in [2], the operations for each layer are defined by a weight matrix $W^i \in \mathbb{R}^{n_i \times n_{i-1}}$, a bias vector $b^i \in \mathbb{R}^{n_i}$, and the activation function $\text{sat}(\cdot)$. Differently from [2], a linear term $Kx(k)$ is added to the output of the NN and we will study its potential later in the chapter.

We can rewrite the closed-loop system (1)-(2) in a compact form with isolated nonlinear functions to separate the linear operations from the nonlinear ones in the neural network [25, 4]. Then, we consider the augmented vectors

$$\begin{aligned}
v_\phi &= [v^1{}^\top \dots v^\ell{}^\top]^\top, \\
\omega_\phi &= [\omega^1{}^\top \dots \omega^\ell{}^\top]^\top, \\
\hat{\omega}_\phi &= [\hat{\omega}^1{}^\top \dots \hat{\omega}^\ell{}^\top]^\top \in \mathbb{R}^{n_\phi},
\end{aligned}$$

with $n_\phi = \sum_{i=1}^\ell n_i$. The i^{th} element of v_ϕ , for instance, is denoted by $v_{\phi,i}$. A combined nonlinearity $\text{sat}(\cdot) : \mathbb{R}^{n_\phi} \rightarrow \mathbb{R}^{n_\phi}$ can also be obtained by stacking all saturation functions, i.e.

$$\omega_\phi(k) = \text{sat}(v_\phi) = [\text{sat}(v^1)^\top \dots \text{sat}(v^\ell)^\top]^\top \in \mathbb{R}^{n_\phi}, \tag{4}$$

The neural network control policy can therefore be described as follows:

$$\begin{bmatrix} u(k) \\ v_\phi(k) \end{bmatrix} = N \begin{bmatrix} x(k) \\ \hat{\omega}_\phi(k) \\ 1 \end{bmatrix}, \tag{5}$$

with

$$N = \left[\begin{array}{c|ccc|c} K & \mathbf{0} & \dots & \mathbf{0} & W^{\ell+1} & b^{\ell+1} \\ \hline W^1 & \mathbf{0} & \dots & \mathbf{0} & \mathbf{0} & b^1 \\ \mathbf{0} & W^2 & \dots & \mathbf{0} & \mathbf{0} & b^2 \\ \vdots & \vdots & \ddots & \vdots & \vdots & \vdots \\ \mathbf{0} & \mathbf{0} & \dots & W^\ell & \mathbf{0} & b^\ell \end{array} \right] = \begin{bmatrix} N_{ux} & N_{u\omega} & N_{ub} \\ N_{vx} & N_{v\omega} & N_{vb} \end{bmatrix}. \tag{6}$$

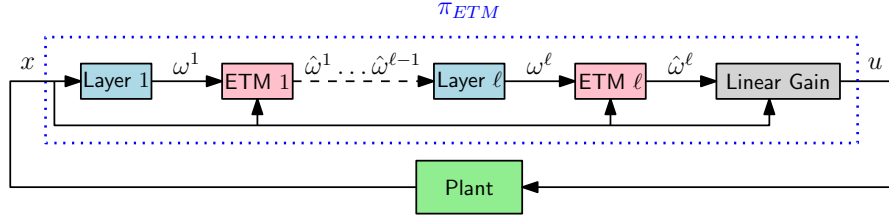


Fig. 1 Control system with event-triggered network controller π_{ETM} .

Remark 1 Differently from [2], it should be noted that $N_{ux} = K \neq \mathbf{0}$ due to the presence of the control gain $K \in \mathbb{R}^{n_u \times n_p}$.

The relation between the current and transmitted outputs $\omega_\phi(k)$ and $\hat{\omega}_\phi(k)$ is described by event-triggering mechanisms (ETMs) located at each layer of the NN: if an event is triggered at instant k at layer i then $\hat{\omega}^i(k) = \omega^i(k)$, otherwise $\hat{\omega}^i(k) = \hat{\omega}^i(k-1)$. The conditions under which events are triggered will be formally introduced in Section 2.3. The overall architecture of our control system is shown in Figure 1.

2.2 Preliminary Model Analysis

It is clear from (4)-(5), that, whenever an event is triggered at layer i , the definition of v_ϕ presents a nonlinear algebraic loop due to the presence of the saturation ($\hat{\omega}^i = \text{sat}(v^i)$) in the right-hand term. With $N_{v\omega} = \mathbf{0}$ one retrieves the classical linear state-feedback case without algebraic loop (see, for example, [22]). Then, let us discuss the aspects related to the nonlinear algebraic loop when $N_{v\omega} \neq \mathbf{0}$. Necessary and sufficient well-posedness conditions can be, for instance, derived from [11, Claim 2]. If the algebraic loop is well-posed then one can guarantee the existence of a (piecewise affine) solution to v_ϕ in (4)-(5). In the particular case considered here, the lower triangular structure of $N_{v\omega}$ ensures that the algebraic loop, and thus the control system, are well posed. Then, we can state the following result regarding the uniform boundedness of the trajectories of the control system:

Lemma 1 Assume that the matrix $A_p + B_p K$ is Schur-Cohn. Then, there exist $\beta, \gamma_x, \gamma_\omega > 0$ such that for all trajectories of the control system, it holds

$$\|x(k)\| \leq \beta + \gamma_x \|x(0)\| + \gamma_\omega \|\hat{\omega}^\ell(0)\|, \quad \forall k \in \mathbb{N}. \quad (7)$$

Proof From the use of bounded activation functions given by saturation maps and of ETMs, we have that for all $k \in \mathbb{N}$, $|\hat{\omega}^\ell(k)| \leq \max(|\hat{\omega}^\ell(0)|, \bar{v}^\ell)$, which implies from (2) that

$$\|u(k) - Kx(k)\| \leq \| |W^{\ell+1}| \max(|\hat{\omega}^\ell(0)|, \bar{v}^\ell) + |b^\ell| \|, \quad \forall k \in \mathbb{N}.$$

Then, (7) follows from the previous inequality and the fact that the matrix $A_p + B_p K$ is Schur-Cohn. \square

Let us now discuss briefly the existence of equilibrium points of (1) and (5)-(6), that we denote $(x_*, u_*, v_*, \omega_*, \hat{\omega}_*)$ with $\omega_* = \hat{\omega}_*$. Then, the following conditions must be satisfied

$$\begin{aligned} x_* &= A_p x_* + B_p u_*, \quad \omega_*^0 = x_*, \\ \begin{bmatrix} u_* \\ v_* \end{bmatrix} &= N \begin{bmatrix} x_* \\ \omega_* \\ 1 \end{bmatrix}, \\ \omega_* &= \text{sat}(v_*). \end{aligned} \tag{8}$$

Then, consider the matrices:

$$\begin{aligned} R &= (\mathbf{I} - N_{v\omega})^{-1} \\ R_\omega &= N_{ux} + N_{u\omega} R N_{vx} = K + N_{u\omega} R N_{vx} \\ R_b &= N_{u\omega} R N_{vb} + N_{ub}. \end{aligned} \tag{9}$$

Note that the lower triangular structure of $N_{v\omega}$ ensures that $\mathbf{I} - N_{v\omega}$ is always invertible. Then, let us make the following assumptions:

Assumption 1 The matrix $\mathbf{I} - A_p - B_p R_\omega$ is invertible.

Assumption 2 $-\bar{v} \leq R N_{vx} [\mathbf{I} - A_p - B_p R_\omega]^{-1} B_p R_b + R N_{vb} \leq \bar{v}$.

Then, we can state the following result:

Lemma 2 *Under Assumptions 1 and 2, there exists a unique equilibrium $(x_*, u_*, v_*, \omega_*, \hat{\omega}_*)$ such that $-\bar{v} \leq v_* \leq \bar{v}$. This equilibrium point is given by*

$$\begin{aligned} x_* &= [\mathbf{I} - A_p - B_p R_\omega]^{-1} B_p R_b, \\ u_* &= R_\omega x_* + R_b, \\ v_* &= R N_{vx} x_* + R N_{vb}, \\ \omega_* &= \hat{\omega}_* = v_*, \end{aligned} \tag{10}$$

with the matrices R , R_ω and R_b defined in (9)

Proof Let us look for an equilibrium point such that $-\bar{v} \leq v_* \leq \bar{v}$, i.e. such that $\text{sat}(v_*) = v_*$. Then, it follows from (6)-(8) and Assumption 1 that such an equilibrium point is unique and given by (10). Then, Assumption 2 ensures that $-\bar{v} \leq v_* \leq \bar{v}$ indeed holds. \square

In the rest of the chapter, we will assume that Assumptions 1 and 2 hold.

2.3 Event-Triggering Mechanism

To reduce the computational cost incurred by the evaluation of the neural network at each time step, the NN architecture is equipped with ETMs located at the outputs

of each layer, as shown in Figure 1. The ETMs decide whether or not to update the current outputs through the neural network.

In this work, we propose to use ETMs given by rules of the following form for $i \in \{1, \dots, \ell\}$:

$$\hat{\omega}^i(k) = \begin{cases} \omega^i(k), & \text{if } f^i(\hat{\omega}^i(k-1), v^i(k), x(k)) > 0, \\ \hat{\omega}^i(k-1), & \text{otherwise,} \end{cases} \quad (11)$$

with $f^i(\hat{\omega}^i(k-1), v^i(k), x(k))$ defined by

$$f^i(\hat{\omega}^i(k-1), v^i(k), x(k)) = [v^i(k) - \hat{\omega}^i(k-1)]^\top T^i [G^i(x(k) - x_*) - (\hat{\omega}^i(k-1) - \omega_*^i)] \quad (12)$$

where $T^i \in \mathbb{R}^{n_i \times n_i}$ is a diagonal positive definite matrix and $G^i \in \mathbb{R}^{n_i \times n_p}$.

We can now provide a statement of the problem under consideration in this paper:

Problem 1 Consider the NN controller π_{ETM} (4)-(5) that stabilizes the plant (1). Design ETMs, according to (11)-(12), i.e. design the matrices T^i , G^i , to reduce the computational cost associated with the evaluation of the neural network while preserving the stability of the control system.

The presence of the saturation functions implies that the control system is non-linear and asymptotic stability of the equilibrium point x_* can be ensured globally (that is for any initial condition $x(0) \in \mathbb{R}^n$) or only locally (that is, only for initial conditions in a neighborhood of x_*). Regional (local) asymptotic stability holds if and only if $A_p + B_p R_\omega$ is Schur, but in that case, the characterization of a large inner approximation of the basin of attraction requires nontrivial derivations (see, e.g., [10], [22], [27]). That constitutes an implicit problem in Problem 1. Hence, a classical trade-off can be considered between the size of the estimate of the region of attraction and the update saving.

Fundamental limitations of bounded stabilization of linear systems [19] imply that when $A_p + B_p K$ has unstable eigenvalues (i.e. outside the unit circle), the maximal set of initial conditions providing solutions that converge to x_* (corresponding to the basin of attraction of x_*) is bounded. The exact characterization of the basin of attraction remains an open problem in general. Hence, a challenging problem consists in computing accurate approximations. A guarantee on the size of the basin of attraction is typically done through an inner approximation, which corresponds to study the regional asymptotic stability.

Let us briefly discuss another important point related to an effective implementation of ETMs (11)-(12). In comparison to [2] or [1] where the ETM at layer i uses only local information (i.e. values of $\hat{\omega}^{i-1}$, $\hat{\omega}^i$, v_i or ω^i), ETM (11)-(12) uses non-local information since the knowledge of the value of $x(k)$ is required. For the ETM at layer i , we define variables $q_i(k) \in \mathbb{R}^{n_p}$, $r_i(k) \in \mathbb{R}$ given by

$$q_i(k) = G^{i\top} T^i [v^i(k) - \hat{\omega}^i(k)],$$

and

$$r_i(k) = [v^i(k) - \hat{\omega}^i(k)]^\top T^i [G^i x_* + (\hat{\omega}^i(k) - \omega_*^i)].$$

Let us remark, that if at time k , an event is not triggered at layer $i - 1$, then

$$f^i(\hat{\omega}^i(k-1), v^i(k), x(k)) = q_i(k-1)^\top x(k) - r_i(k-1).$$

The triggering condition (11) can then be checked much more efficiently than using (12) particularly when the dimension of the state n_p is much smaller than the number of neurons in the layer n_i . Moreover, it is to be noted that if no event is triggered at layer $i - 1$ nor at layer i then we have $q_i(k) = q_i(k-1)$ and $r_i(k) = r_i(k-1)$. Thus, these variables only need to be updated when events are triggered at layer $i - 1$ or at layer i .

3 LMI-based Design of ETM

In this section, we propose an approach to solve Problem 1 based on solving an optimization problem given by linear matrix inequalities (LMIs). We first show how the nonlinear activation functions can be abstracted by quadratic constraints. Then, we establish sufficient conditions for stability under the form of LMIs. Then, we discuss the optimization procedure required to compute a solution to these LMIs.

3.1 Activation Functions as Quadratic Constraints

We consider activation functions given by saturation maps. Thus, we have the following property adapted from [22, Lemma 1.6, page 43], see also [2]:

Lemma 3 For $i \in \{1, \dots, \ell\}$, consider a matrix $G^i \in \mathbb{R}^{n_i \times n_p}$. If $x(k)$ belongs to the set \mathcal{S}^i defined by

$$\mathcal{S}^i = \{x(k) \in \mathbb{R}^{n_p} : -\bar{v}^i - v_*^i \leq G^i(x(k) - x_*) \leq \bar{v}^i - v_*^i\}$$

then, the following quadratic constraint holds:

$$[v^i(k) - \omega^i(k)]^\top T^i [G^i(x(k) - x_*) - (\omega^i(k) - \omega_*^i)] \leq 0 \quad (13)$$

for any diagonal positive definite matrix $T^i \in \mathbb{R}^{n_i \times n_i}$.

Proof If $x(k)$ is an element of \mathcal{S}^i , it follows that for all $j \in \{1, \dots, n_i\}$, $G_j^i(x(k) - x_*) - (-\bar{v}_j^i - v_{*,j}^i) \geq 0$ and $G_j^i(x(k) - x_*) - (\bar{v}_j^i - v_{*,j}^i) \leq 0$. Consider now the three cases below.

- Case 1: $v_j^i(k) \geq \bar{v}_j^i$. It follows that $v_j^i(k) - \omega_j^i(k) = v_j^i(k) - \bar{v}_j^i \geq 0$ and that $G_j^i(x(k) - x_*) - (\omega_j^i(k) - \omega_{*,j}^i) = G_j^i(x(k) - x_*) - (\bar{v}_j^i - v_{*,j}^i) \leq 0$. Then, one

gets

$$\left[v_j^i(k) - \omega_j^i(k) \right] \times \left[G_j^i(x(k) - x_*) - (\omega_j^i(k) - \omega_{*,j}^i) \right] \leq 0. \quad (14)$$

- Case 2: $v_j^i(k) \leq -\bar{v}_j^i$. It follows that $v_j^i(k) - \omega_j^i(k) = v_j^i(k) + \bar{v}_j^i \leq 0$ and that $G_j^i(x(k) - x_*) - (\omega_j^i(k) - \omega_{*,j}^i) = G_j^i(x(k) - x_*) - (-\bar{v}_j^i - v_{*,j}^i) \geq 0$. Then, one gets (14).
- Case 3: $-\bar{v}_i < v_{\phi,i} < \bar{v}_i$. It follows that $v_j^i(k) - \omega_j^i(k) = 0$ and one gets (14).

Since (14) holds for all $j \in \{1, \dots, n_i\}$, we get that (13) holds for all diagonal positive definite matrix T^i . \square

Remark 2 Note that relation (13) can be rewritten equivalently as:

$$\left[(v^i(k) - v_*^i) - (\omega^i(k) - \omega_*^i) \right]^\top T^i \left[G^i(x(k) - x_*) - (\omega^i(k) - \omega_*^i) \right] \leq 0 \quad (15)$$

since by Lemma 2 one gets $v_* = \omega_*$.

From the previous Lemma, we can deduce that a quadratic constraint is enforced by the ETM (11)-(12).

Proposition 1 Consider matrices $G = [G^{1\top} \dots G^{\ell\top}]^\top$ with $G^i \in \mathbb{R}^{n_i \times n_p}$, $i \in \{1, \dots, \ell\}$ and $T = \text{diag}(T^1 \dots T^\ell)$ with $T^i \in \mathbb{R}^{n_i \times n_i}$, $i \in \{1, \dots, \ell\}$ diagonal positive definite matrices. Consider NN controller π_{ETM} (4)-(5) with ETM (11)-(12). Under Assumption 1, if $x(k)$ belongs to the set \mathcal{S} defined by

$$\mathcal{S} = \{x(k) \in \mathbb{R}^{n_p} : -\bar{v} - v_* \leq G(x(k) - x_*) \leq \bar{v} - v_*\}$$

then, the following quadratic constraint holds:

$$\left[v_\phi(k) - \hat{\omega}_\phi(k) \right]^\top T \left[G(x(k) - x_*) - (\hat{\omega}_\phi(k) - \omega_*) \right] \leq 0. \quad (16)$$

Proof Since T is a diagonal matrix, it follows that (16) holds if and only if the following hold for all $i \in \{1, \dots, \ell\}$

$$\left[v^i(k) - \hat{\omega}^i(k) \right]^\top T^i \left[G^i(x(k) - x_*) - (\hat{\omega}^i(k) - \omega_*^i) \right] \leq 0. \quad (17)$$

Then, let us consider two possible cases according to (11). If $\hat{\omega}^i(k) = \omega^i(k)$, then since $x(k) \in \mathcal{S} \subseteq \mathcal{S}^i$, we obtain (17) from (13) in Lemma 3. If $\hat{\omega}^i(k) \neq \omega^i(k)$ then we get from (11)-(12) that $\hat{\omega}^i(k) = \hat{\omega}^i(k-1)$ and that

$$\left[v^i(k) - \hat{\omega}^i(k-1) \right]^\top T^i \left[G^i(x(k) - x_*) - (\hat{\omega}^i(k-1) - \omega_*^i) \right] \leq 0,$$

which gives us (17). \square

Here, it should be highlighted that the particular form of the ETM (11)-(12) has been chosen such that the quadratic constraint used to abstract the nonlinear activation functions are satisfied at all time. This particular construction of ETMs has already been considered in the case of different activation functions in [1].

3.2 Sufficient Conditions for Stability

In this section, we establish sufficient conditions under the form of LMIs that guarantee the regional (local) asymptotic stability of the control system and provide an estimate of the basin of attraction of the equilibrium point.

For further discussions, we introduce the auxiliary variable $\psi_\phi(k) = v_\phi(k) - \hat{\omega}_\phi(k)$. Let us remark that at the equilibrium $\psi_* = v_* - \hat{\omega}_* = 0$. Moreover, from Proposition 1, we get that if $x(k)$ belongs to the set \mathcal{S} , then

$$\psi_\phi(k)^\top T [G(x(k) - x_*) + (\psi_\phi(k) - v_\phi(k) - \psi_* + v_*)] \leq 0. \quad (18)$$

Moreover, we can write the control system in the following compact form:

$$\begin{aligned} x(k+1) &= (A_p + B_p R_\omega)x(k) - B_p N_{u\omega} R \psi_\phi(k) + B_p R_b \\ v_\phi(k) &= R N_{vx} x(k) + (\mathbf{I} - R) \psi_\phi(k) + R N_{vb} \end{aligned} \quad (19)$$

with matrices R , R_ω and R_b defined in (9). Let us define the matrices

$$R_\phi = \begin{bmatrix} \mathbf{I} & \mathbf{0} \\ R N_{vx} & \mathbf{I} - R \\ \mathbf{0} & \mathbf{I} \end{bmatrix}, \bar{A}_p = A_p + B_p R_\omega = A_p + B_p K + B_p N_{u\omega} R N_{vx}. \quad (20)$$

Theorem 1 Consider the control system given by the plant (1), the NN controller π_{ETM} (4)-(5). Assume that there exist a symmetric positive definite matrix $P \in \mathbb{R}^{n_p \times n_p}$, a diagonal positive definite matrix $T = \text{diag}(T^1 \dots, T^\ell)$ with $T^i \in \mathbb{R}^{n_i \times n_i}$, $i \in \{1, \dots, \ell\}$, a matrix $Z = [Z^{1\top} \dots Z^{\ell\top}]^\top$, $Z^i \in \mathbb{R}^{n_i \times n_p}$, $i \in \{1, \dots, \ell\}$, and a scalar $0 < \alpha \in \mathbb{R}$, such that the following matrix inequalities hold

$$\begin{bmatrix} \bar{A}_p^\top \\ (-B_p N_{u\omega} R)^\top \end{bmatrix} P [\bar{A}_p - B_p N_{u\omega} R] - \begin{bmatrix} P & \mathbf{0} \\ \mathbf{0} & \mathbf{0} \end{bmatrix} - R_\phi^\top \begin{bmatrix} \mathbf{0} & Z^\top \\ \mathbf{0} & -T \\ \mathbf{0} & T \end{bmatrix} - \begin{bmatrix} \mathbf{0} & \mathbf{0} & \mathbf{0} \\ Z & -T & T \end{bmatrix} R_\phi < \mathbf{0}, \quad (21)$$

$$\begin{bmatrix} P & Z_j^{i\top} \\ \star & 2\alpha T_{j,j}^i - \alpha^2 (\hat{v}_j^i)^{-2} \end{bmatrix} \geq \mathbf{0}, \quad \forall i \in \{1, \dots, \ell\}, j \in \{1, \dots, n_i\} \quad (22)$$

where $\hat{v}_j^i = \min(|-\bar{v}_j^i - v_{*,j}^i|, |\bar{v}_j^i - v_{*,j}^i|)$. Let the parameters of the ETMs (11)-(12) be given by T and $G_j = (T_{j,j})^{-1} Z_j$. Then:

1. the control system is locally stable around x_* ,
2. the set $\mathcal{E}(P, x_*) = \{x \in \mathbb{R}^{n_F} : (x - x_*)^\top P (x - x_*) \leq 1\}$ is an estimate of the domain of attraction for the control system.

Proof The proof mimics that one in [2]. Consider the candidate Lyapunov function as $V(x(k)) = (x(k) - x_*)^\top P (x(k) - x_*)$ with $\mathbf{0} < P = P^\top \in \mathbb{R}^{n_p \times n_p}$. First, note that from the definition of R_ϕ in (20), it follows that

$$\begin{bmatrix} x(k) - x_* \\ v_\phi(k) - v_* \\ \psi_\phi(k) - \psi_* \end{bmatrix} = R_\phi \begin{bmatrix} x(k) - x_* \\ \psi_\phi(k) - \psi_* \end{bmatrix}$$

which allows us to re-write condition (18) as

$$\begin{bmatrix} x(k) - x_* \\ \psi_\phi(k) - \psi_* \end{bmatrix}^\top \begin{bmatrix} \mathbf{0} \\ \mathbf{I} \end{bmatrix} T [G \ -\mathbf{I} \ \mathbf{I}] R_\phi \begin{bmatrix} x(k) - x_* \\ \psi_\phi(k) - \psi_* \end{bmatrix} \leq 0 \quad (23)$$

Assume the feasibility of relation (22), use the inequality $[\alpha \hat{v}_i^{-2} - T_{i,i}] \hat{v}_i^2 [\alpha \hat{v}_i^{-2} - T_{i,i}] \geq 0$ or equivalently $T_{i,i}^2 \hat{v}_i^2 \geq 2\alpha T_{i,i} - \alpha^2 \hat{v}_i^{-2}$ and consider the change of variables $G_j = (T_{j,j})^{-1} Z_j$. Then relation (22) reads

$$\begin{bmatrix} P & G_j^\top T_{j,j} \\ \star & T_{j,j}^2 \hat{v}_j^2 \end{bmatrix} \geq \mathbf{0}, \quad \forall j \in \{1, \dots, n_i\}.$$

That corresponds to ensure

$$(x - x_*)^\top G_i^\top \hat{v}_i^{-2} G_j (x - x_*) \leq (x - x_*)^\top P (x - x_*)$$

which ensures that $\mathcal{E}(P, x_*) \subseteq \mathcal{S}$, consequently, Lemma 3 applies. As the bounds of the set \mathcal{S} are asymmetric, one considers the minimal bound in absolute value: $\hat{v}_i = \min(|-\bar{v}_i - v_{*,i}|, |\bar{v}_i - v_{*,i}|)$.

Consider that condition (21) holds, then there exists a scalar $\epsilon > 0$ such that pre and post multiplying (21) by $[(x(k) - x_*)^\top (\psi_\phi(k) - \psi_*)^\top]$ and its transpose, respectively, it holds

$$\begin{aligned} & \begin{bmatrix} x(k) - x_* \\ \psi_\phi(k) - \psi_* \end{bmatrix}^\top \left(\begin{bmatrix} \bar{A}_p^\top \\ (-B_p N_{u\omega} R)^\top \end{bmatrix} P [\bar{A}_p \ -B_p N_{u\omega} R] - \begin{bmatrix} P & \mathbf{0} \\ \mathbf{0} & \mathbf{0} \end{bmatrix} \right. \\ & \left. - R_\phi^\top \begin{bmatrix} \mathbf{0} & Z^\top \\ \mathbf{0} & -T \\ \mathbf{0} & T \end{bmatrix} - \begin{bmatrix} \mathbf{0} & \mathbf{0} & \mathbf{0} \\ Z & -T & T \end{bmatrix} R_\phi \right) \begin{bmatrix} x(k) - x_* \\ \psi_\phi(k) - \psi_* \end{bmatrix} < -\epsilon \|x(k) - x_*\|^2. \quad (24) \end{aligned}$$

Then, replacing Z by TG , and rearranging terms by taking into account the definition of the closed loop in (19), yields:

$$\begin{aligned} \Delta V(x(k)) - 2 \begin{bmatrix} x(k) - x_* \\ \psi_\phi(k) - \psi_* \end{bmatrix}^\top \begin{bmatrix} \mathbf{0} \\ \mathbf{I} \end{bmatrix} T [G \ -\mathbf{I} \ \mathbf{I}] R_\phi \begin{bmatrix} x(k) - x_* \\ \psi_\phi(k) - \psi_* \end{bmatrix} \\ < -\epsilon \|x(k) - x_*\|^2 \quad (25) \end{aligned}$$

with $\Delta V(x(k)) = V(x(k+1)) - V(x(k)) = (x(k+1) - x_*)^\top P (x(k+1) - x_*) - (x(k) - x_*)^\top P (x(k) - x_*)$.

By invoking (23), we can conclude that if $x(k)$ belongs to the set \mathcal{S} , then

$$\begin{aligned} \Delta V(x(k)) &\leq \\ \Delta V(x(k)) - 2 \begin{bmatrix} x(k) - x_* \\ \psi_\phi(k) - \psi_* \end{bmatrix}^\top &\begin{bmatrix} \mathbf{0} \\ \mathbf{I} \end{bmatrix} T [G \ -\mathbf{I} \ \mathbf{I}] R_\phi \begin{bmatrix} x(k) - x_* \\ \psi_\phi(k) - \psi_* \end{bmatrix} \\ &< -\epsilon \|x(k) - x_*\|^2. \end{aligned} \quad (26)$$

Inequality (26) implies that if $x(k) \in \mathcal{E}(P, x_*)$ then $x(k+1) \in \mathcal{E}(P, x_*)$ (i.e. $\mathcal{E}(P, x_*)$ is an invariant set) and $x(k)$ converges to the equilibrium point x_* . Therefore, $\mathcal{E}(P, x_*)$ is an inner-approximation of the domain of attraction of x_* for the closed-loop system. The proof is complete. \square

If matrix $A_p + B_p K$ is Schur-Cohn, Theorem 1 may also be considered in a global context.

Theorem 2 Consider the control system given by the plant (1), the NN controller π_{ETM} (4)-(5). Assume that there exist a symmetric positive definite matrix $P \in \mathbb{R}^{n_p \times n_p}$, a diagonal positive definite matrix $T = \text{diag}(T^1 \dots, T^\ell)$ with $T^i \in \mathbb{R}^{n_i \times n_i}$, $i \in \{1, \dots, \ell\}$ such that the following matrix inequality holds

$$\begin{bmatrix} \bar{A}_p^\top \\ (-B_p N_{u\omega} R)^\top \end{bmatrix} P [\bar{A}_p - B_p N_{u\omega} R] - \begin{bmatrix} P & \mathbf{0} \\ \mathbf{0} & \mathbf{0} \end{bmatrix} - R_\phi^\top \begin{bmatrix} \mathbf{0} & \mathbf{0} \\ \mathbf{0} & -T \\ \mathbf{0} & T \end{bmatrix} - \begin{bmatrix} \mathbf{0} & \mathbf{0} & \mathbf{0} \\ \mathbf{0} & -T & T \end{bmatrix} R_\phi < \mathbf{0}. \quad (27)$$

Then the equilibrium point x_* is globally asymptotically stable for the closed loop.

Proof The proof follows the same reasoning as that one of Theorem 1. In the global case Lemma 3 is applied by choosing $G = \mathbf{0}$ [22]. Hence, relation (22) disappears and relation (21) is rewritten as in (27). The satisfaction of this condition means that one gets

$$\begin{aligned} \Delta V(x(k)) &\leq \\ \Delta V(x(k)) - 2 \begin{bmatrix} x(k) - x_* \\ \psi_\phi(k) - \psi_* \end{bmatrix}^\top &\begin{bmatrix} \mathbf{0} \\ \mathbf{I} \end{bmatrix} T [\mathbf{0} \ -\mathbf{I} \ \mathbf{I}] R_\phi \begin{bmatrix} x(k) - x_* \\ \psi_\phi(k) - \psi_* \end{bmatrix} \\ &< -\epsilon \|x(k) - x_*\|^2. \end{aligned} \quad (28)$$

In other words, $x(k)$ globally converges to the equilibrium point x_* and the proof is complete. \square

In order to better understand the necessary assumption on the stability of matrix $A = A_p + B_p K$, one can study the feasibility of condition (27). To do this one can rewrite condition (27) as follows:

$$\begin{bmatrix} \bar{A}_p^\top \\ (-B_p N_{u\omega} R)^\top \end{bmatrix} P [\bar{A}_p - B_p N_{u\omega} R] - \begin{bmatrix} P & \mathbf{0} \\ \mathbf{0} & \mathbf{0} \end{bmatrix} + He\left\{ \begin{bmatrix} \mathbf{0} \\ \mathbf{I} \end{bmatrix} T [R N_{vx} - R] \right\} < \mathbf{0}. \quad (29)$$

By pre- and post-multiplying (29) by $\begin{bmatrix} \mathbf{I} & N_{yx}^\top \\ \mathbf{0} & \mathbf{I} \end{bmatrix}$ and $\begin{bmatrix} \mathbf{I} & \mathbf{0} \\ N_{yx} & \mathbf{I} \end{bmatrix}$, one gets

$$\begin{bmatrix} (A_p + B_p K)^\top \\ (-B_p N_{u\omega} R)^\top \end{bmatrix} P \begin{bmatrix} (A_p + B_p K) & -B_p N_{u\omega} R \end{bmatrix} - \begin{bmatrix} P & \mathbf{0} \\ \mathbf{0} & \mathbf{0} \end{bmatrix} + He \left\{ \begin{bmatrix} N_{yx}^\top \\ \mathbf{I} \end{bmatrix} T \begin{bmatrix} \mathbf{0} & -R \end{bmatrix} \right\} < \mathbf{0}.$$

Note that the block $(1, 1)$ of the expression above is $(A_p + B_p K)^\top P (A_p + B_p K) - P$. Hence, it is clear that a necessary condition for the feasibility of (29), or equivalently for (27), is to have $(A_p + B_p K)^\top P (A_p + B_p K) - P < \mathbf{0}$. That corresponds to have the assumption that the matrix $A_p + B_p K$ is Schur-Cohn.

3.3 Optimization Procedure

Let us first provide some comments regarding conditions (21) and (22). Condition (21) is linear in the decision variables P , T and Z , whereas condition (22) is only linear in P but not in T and α . However, condition (22) will become linear if we fix α .

In this section, an optimization scheme is proposed to reduce the evaluation activity in the neural network, but taking into account the trade-off between the update saving and the size of the inner approximation of the region of attraction of x_* . Then, consider $\mathcal{X}_0 = \mathcal{E}(P_0, x_*) = \{x \in \mathbb{R}^{n_p} : (x - x_*)^\top P_0 (x - x_*) \leq 1\}$, with $\mathbf{0} < P_0^\top = P_0 \in \mathbb{R}^{n_p \times n_p}$, a set to be contained in the region of attraction of the closed-loop system, i.e. $\mathcal{X}_0 \subseteq \mathcal{E}(P, x_*)$. Then the inclusion is obtained by imposing

$$\begin{bmatrix} P_0 & P \\ P & P \end{bmatrix} \geq \mathbf{0}. \quad (30)$$

Then, by taking inspiration of [2], the following optimization scheme that can help to enlarge such an estimate, while reducing the amount of computation:

$$\begin{aligned} & \min \rho \\ & \text{subject to (21), (22), (30), } M_1 \geq -\rho \mathbf{I} \end{aligned} \quad (31)$$

with $\rho > 0$ and M_1 is the matrix defined in the left-hand term of (21).

By considering the optimization problem (31) we are trying to indirectly 1) maximizing the inner approximation of the region of attraction, and 2) approaching the infeasibility of the stability condition.

4 Simulations

Consider the inverted pendulum system with mass $m = 0.15 \text{ kg}$, length $l = 0.5 \text{ m}$, and friction coefficient $\mu = 0.5 \text{ Nms/rad}$. The following discrete-time model describes

its dynamics:

$$\begin{bmatrix} x_1(k+1) \\ x_2(k+1) \end{bmatrix} = \begin{bmatrix} 1 & \delta \\ \frac{g\delta}{l} & 1 - \frac{\delta\mu}{ml^2} \end{bmatrix} \begin{bmatrix} x_1(k) \\ x_2(k) \end{bmatrix} + \begin{bmatrix} 0 \\ \frac{\delta}{ml^2} \end{bmatrix} u(k), \quad (32)$$

where the states $x_1(k)$ and $x_2(k)$ represent respectively the angular position (rad) and velocity (rad/s), $u(k)$ is the control input (Nm) and $\delta = 0.02$ is the sampling time [26].

To stabilize (32), we have designed a controller π under the form of a 2-layer, feedforward neural network, with $n_1 = n_2 = 32$, the saturation as the activation function for both layers, and a linear term $Kx(k)$ in the output of the neural network. For training purpose only, we replaced the saturation by its smooth approximation provided by \tanh , making it possible to rely on MATLAB's Reinforcement Learning toolbox. During the training, the agent's decision is characterized by a Gaussian distribution probability with mean $\pi(x(k))$ and standard deviation σ . In addition, to illustrate the applicability of our condition to equilibrium points different from 0, we have not set the bias in neural network to zero during training. After training, the policy mean π is used as the deterministic controller $u(k) = \pi(x(k))$ with the saturation as the activation function.

First, we have designed the ETMs (11)-(12) for 3 different linear gains K to show the influence of these gains on the transmission saving and the size of the estimate of the region of attraction. In this case, by setting $\bar{v} = -\underline{v} = 1 \times 1_{64 \times 1}$, we use the optimization procedure (31) with

$$P_0 = \begin{bmatrix} 0.2916 & 0.0054 \\ \star & 0.0090 \end{bmatrix}, \quad (33)$$

chosen based on the maximum estimate of the region of attraction obtained without trigger and $\alpha = 9 \times 10^{-4}$. Then, we simulate the feedback system for 100 initial conditions belonging to the estimates of the region of attraction. The results are shown in Table 1.

Gains	1st Layer	2nd Layer	Area
$K = [-0.1 \ 0]$	23.05%	22.61%	111.22
$K = [-0.3 \ 0]$	21.20%	20.67%	126.17
$K = [-0.5 \ 0]$	18.61%	17.97%	135.45

Table 1 Comparison of update rates (columns 2 and 3) and $\mathcal{E}(P, x_*)$ areas (column 4) achieved with optimization procedure (31) for different gains K .

To illustrate, considering the first gain, $K = [-0.1 \ 0]$, we have plotted in Figure 2 the state trajectories and the control signals of the feedback system for the 100 initial conditions belonging to the boundary of the estimate of region of attraction. Also,

by considering the initial conditions $x_0 = [-1.8341 \ -6.9559]^\top$, we have plotted in the top of Figure 3, the inter-event time of both layers ω^1 and ω^2 and in the middle and bottom, the outputs of the first neuron of each layer, respectively. We can see that all curves converge to their respective equilibrium points with an update rate of 23.71% and 22.29% for ω^1 and ω^2 , respectively, thus reducing the computational cost associated with the control law evaluation. In addition, it is possible to see that ω_1^2 saturates in the first instants of simulation.

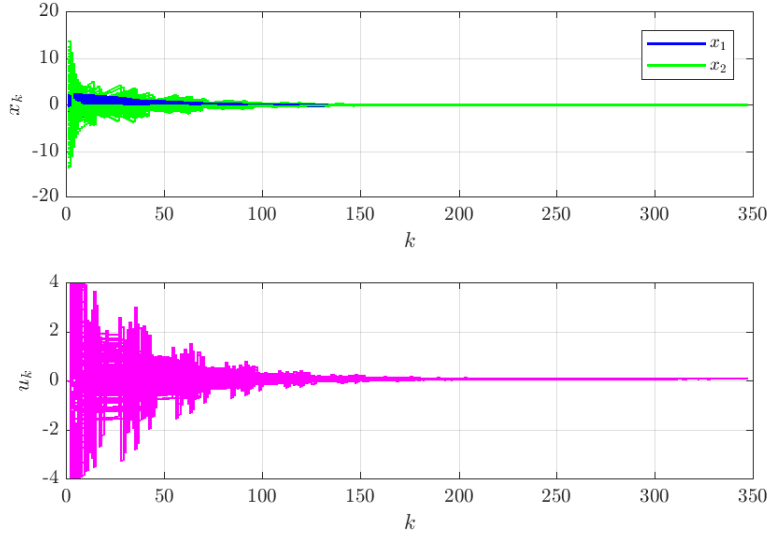


Fig. 2 The feedback response of the system using $K = [-0.1 \ 0]$ for different initial conditions in the border of the $\mathcal{E}(P, x_*)$. Top: system' states; bottom: control signal computed (blue-line).

Moreover, figures 4, 5 and 6, depict respectively for each gain in Table 1, the estimate of the region of attraction $\mathcal{E}(P, x_*)$ (blue solid line) and the set of admissible initial states $\mathcal{E}(P_0, x_*)$ (red solid line). Some convergent and divergent trajectories are also shown in cyan dashed lines and green dash-dotted lines, starting from the points marked with cyan circles and green asterisks, respectively. Note that in all cases the estimate of the region of attraction does not overstep the bounds $\{-\bar{\nu} - \nu_* \leq G(x - x_*) \leq \bar{\nu} - \nu_*\}$ (orange lines) for both layers, as expected. Also, we can verify that as the absolute value of the gain increases, the size of the estimate of the region of attraction increases, which can be verified in the last column of Table 1, which shows the area of the ellipses $\mathcal{E}(P, x_*)$. Note that the estimate of the region of attraction increased 13.44% and 21.78%, respectively, in relation to the first case.

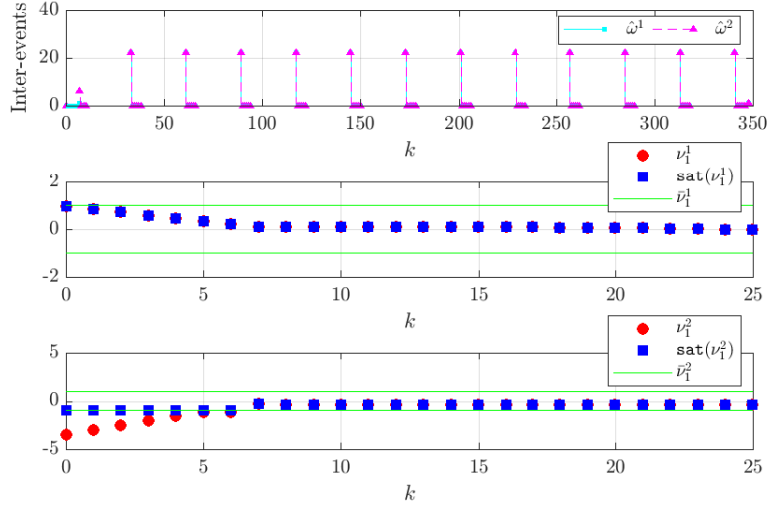


Fig. 3 Top: Inter-event time of both layers ω^1 and ω^2 ; Middle and bottom: Outputs of the first neuron of each layer; for $K = \begin{bmatrix} -0.1 & 0 \end{bmatrix}$ and $x_0 = \begin{bmatrix} -1.8341 & -6.9559 \end{bmatrix}^\top$.

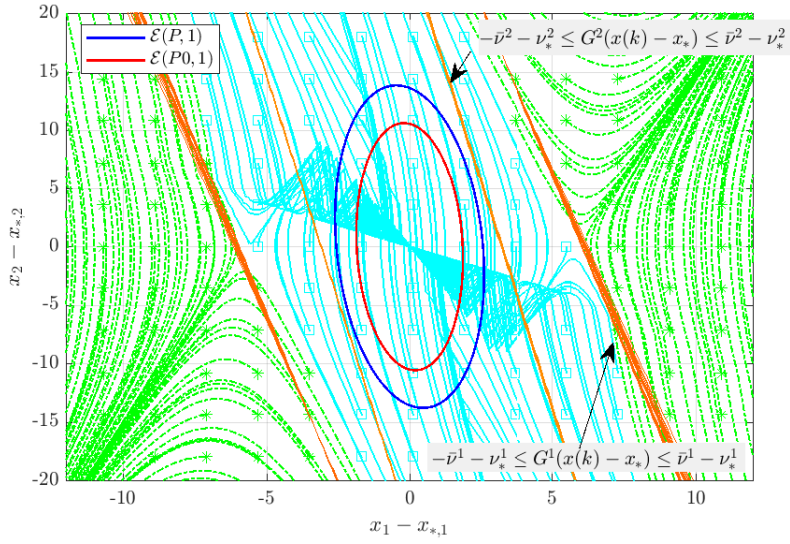


Fig. 4 Estimate of the region of attraction for the feedback system in the plan $(x_1 - x_{*,1} \times x_2 - x_{*,2})$ for $K = \begin{bmatrix} -0.1 & 0 \end{bmatrix}$.

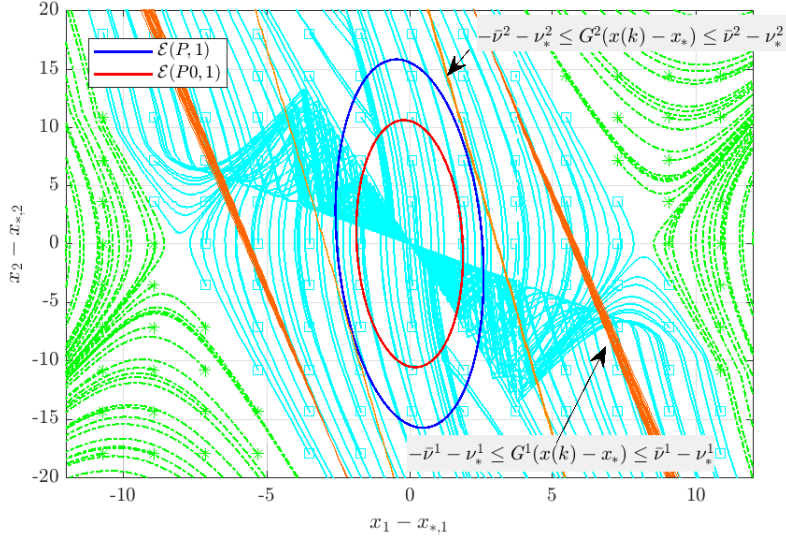


Fig. 5 Estimate of the region of attraction for the feedback system in the plan $(x_1 - x_{*,1} \times x_2 - x_{*,2})$ for $K = [-0.3 \ 0]$.

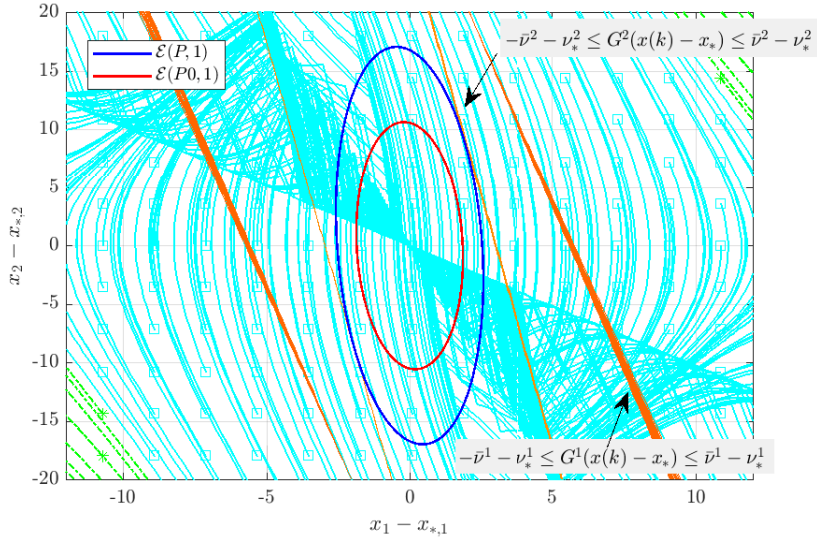


Fig. 6 Estimate of the region of attraction for the feedback system in the plan $(x_1 - x_{*,1} \times x_2 - x_{*,2})$ for $K = [-0.5 \ 0]$.

5 Conclusion

This chapter proposed an event-triggering strategy, based on (local) sectors conditions related to the activation functions in order to decide whether the outputs of the layers should be transmitted through the network or not. This chapter can be viewed as an extension of our previous works [1] and [2]. Theoretical conditions allowed to design the event-triggering mechanism and to estimate the region of attraction, while preserving the stability of the closed-loop system. Simulations have illustrated the effectiveness of the event-triggering scheme, showing a significant reduction of the transmission activity in the neural network even if the number of layer increase. The results open the doors for future works as studying other event-triggering structures and different abstractions in order to reduce the conservatism of the conditions. Another interesting direction could be to study co-design problem, that is, design in the same time the neural network and the event-triggering mechanism.

References

1. C. De Souza, A. Girard, and S. Tarbouriech. Event-triggered neural network control using quadratic constraints for perturbed systems. *Automatica*, 2023. to appear.
2. C. de Souza, S. Tarbouriech, and A. Girard. Event-triggered neural network control for lti systems. *IEEE Control Systems Letters*, 7:1381–1386, 2023.
3. C. de Souza, S. Tarbouriech, V. J. S. Leite, and E. B. Castelan. Co-design of an event-triggered dynamic output feedback controller for discrete-time LPV systems with constraints. *Journal of The Franklin Institute*, 2020. Submitted.
4. M. Fazlyab, M. Morari, and G. J. Pappas. Safety verification and robustness analysis of neural networks via quadratic constraints and semidefinite programming. *IEEE Transactions on Automatic Control*, 2020.
5. M. Fazlyab, A. Robey, H. Hassani, M. Morari, and G. Pappas. Efficient and accurate estimation of lipschitz constants for deep neural networks. *Advances in Neural Information Processing Systems*, 32, 2019.
6. Y. Gao, X. Guo, R. Yao, W. Zhou, and C. Cattani. Stability analysis of neural network controller based on event triggering. *Journal of the Franklin Institute*, 357(14):9960–9975, 2020.
7. A. Girard. Dynamic triggering mechanisms for event-triggered control. *IEEE Transactions on Automatic Control*, 60(7):1992–1997, 2014.
8. W. P. M. H. Heemels, M. C. F. Donkers, and A. R. Teel. Periodic event-triggered control for linear systems. *IEEE Transactions on automatic control*, 58(4):847–861, 2012.
9. M. Hertneck, J. Köhler, S. Trimpe, and F. Allgöwer. Learning an approximate model predictive controller with guarantees. *IEEE Control Systems Letters*, 2(3):543–548, 2018.
10. T. Hu and Z. Lin. *Control Systems with Actuator Saturation: Analysis and Design*. Birkhäuser, Boston, 2001.
11. T. Hu, A.R. Teel, and L. Zaccarian. Stability and performance for saturated systems via quadratic and nonquadratic Lyapunov functions. *IEEE Transactions on Automatic Control*, 51(11):1770–1786, 2006.
12. M. Jin and J. Lavaei. Stability-certified reinforcement learning: A control-theoretic perspective. *IEEE Access*, 8:229086–229100, 2020.
13. B. Karg and S. Lucia. Efficient representation and approximation of model predictive control laws via deep learning. *IEEE Transactions on Cybernetics*, 50(9):3866–3878, 2020.
14. K.-K. K. Kim, E. R. Patrón, and R.D. Braatz. Standard representation and unified stability analysis for dynamic artificial neural network models. *Neural Networks*, 98:251–262, 2018.

15. P. Pauli, A. Koch, J. Berberich, P. Kohler, and F. Allgöwer. Training robust neural networks using lipschitz bounds. *IEEE Control Systems Letters*, 6:121–126, 2021.
16. P. Pauli, J. Köhler, J. Berberich, A. Koch, and F. Allgöwer. Offset-free setpoint tracking using neural network controllers. In *Learning for Dynamics and Control*, pages 992–003. PMLR, 2021.
17. M. Revay, R. Wang, and I. R. Manchester. Lipschitz bounded equilibrium networks. *arXiv preprint arXiv:2010.01732*, 2020.
18. A. Sahoo, H. Xu, and S. Jagannathan. Neural network-based event-triggered state feedback control of nonlinear continuous-time systems. *IEEE Transactions on Neural Networks and Learning Systems*, 27(3):497–509, 2015.
19. W.E. Schmitendorf and B.R. Barmish. Null controllability of linear systems with constrained controls. *SIAM J. Contr. Opt.*, 18(4):327–345, 1980.
20. P. Tabuada. Event-triggered real-time scheduling of stabilizing control tasks. *IEEE Transactions on Automatic Control*, 52(9):1680–1685, 2007.
21. K. Tanaka. An approach to stability criteria of neural-network control systems. *IEEE Transactions on Neural Networks*, 7(3):629–642, 1996.
22. S. Tarbouriech, G. Garcia, J. M. Gomes da Silva Jr., and I. Queinnec. *Stability And Stabilization Of Linear Systems With Saturating Actuators*. Springer, 2011.
23. K. G. Vamvoudakis. Event-triggered optimal adaptive control algorithm for continuous-time nonlinear systems. *IEEE/CAA Journal of Automatica Sinica*, 1(3):282–293, 2014.
24. W. Xiang, P. Musau, A. A. Wild, D. M. Lopez, N. Hamilton, X. Yang, J. Rosenfeld, and T. T. Johnson. Verification for machine learning, autonomy, and neural networks survey. *arXiv preprint arXiv:1810.01989*, 2018.
25. H. Yin, P. Seiler, and M. Arcak. Stability analysis using quadratic constraints for systems with neural network controllers. *IEEE Transactions on Automatic Control*, 2021.
26. H. Yin, P. Seiler, M. Jin, and M. Arcak. Imitation learning with stability and safety guarantees. *IEEE Control Systems Letters*, 6:409–414, 2021.
27. L. Zaccarian and A. R. Teel. *Modern anti-windup synthesis: control augmentation for actuator saturation*, volume 36. Princeton University Press, 2011.
28. X. Zhang, M. Bujarbaruah, and F. Borrelli. Safe and near-optimal policy learning for model predictive control using primal-dual neural networks. In *American Control Conference (ACC)*, pages 354–359. IEEE, 2019.
29. X. Zhong, Z. Ni, H. He, X. Xu, and D. Zhao. Event-triggered reinforcement learning approach for unknown nonlinear continuous-time system. In *International Joint Conference on Neural Networks (IJCNN)*, pages 3677–3684. IEEE, 2014.

Index

A

activation function 2, 4
activation functions 9

B

basin of attraction 7, 10

E

event-triggered control 2
event-triggering mechanism 1, 3, 5

G

globally asymptotically stable 12

L

linear matrix inequalities 8

N

neural network 1–4, 13

Q

quadratic constraints 2, 8

R

regional asymptotic stability 7, 10

S

saturation 2, 4, 7